Importance of dynamical effects for the formation of fragments of 10.7*A* GeV gold nuclei

Khaled Abdel-Waged*
Physics Department, Faculty of Science, Benha University, Benha, Egypt
(Received 14 April 2000; published 25 January 2001)

The correlations between the charges emitted in the collision of 10.7*A* GeV Au nuclei on emulsion targets are analyzed by a multistep model as follows: (i) Glauber scattering at the first stage of the interaction; (ii) dynamical evolution of highly excited fragments; and (iii) statistical decay of the excited residues. The combined model with soft equation of state parameters describes well such correlations, without any adjustments. A comparison between our results and the ones previously obtained by a cascade model indicates that dynamics play a very important role in determining correctly both the excitation energies and source sizes of fragments before final breakup.

DOI: 10.1103/PhysRevC.63.024618 PACS number(s): 25.70.Mn, 24.10.Lx, 24.10.Pa

I. INTRODUCTION

The breakup of heavy nuclei into several pieces, i.e., nuclear multifragmentation (MF), is one of the central interests in reaction physics because the observation of MF is a good tool to study the dynamics and statistics of violent heavy-ion collisions [1–7]. The theoretical description of nuclear MF has traditionally been thought to be a two-step process consisting of the formation of the excited residual nuclei through a quasielastic collision followed by a breakup of the excited residues. Many theoretical investigations, including cascade models [8,9], new types of microscopic simulation theories such as Boltzmann-Uhling-Uhlenbeck (BUU) [10], quantum molecular dynamics (QMD) [11], and relativistic QMD [12], can be used to describe the first fast stage of the interactions. However, most of these models are inapplicable at high energy ($\geqslant$10.7*A* GeV). The cascade model, as shown in Ref. [13], considerably overestimates the breakup of Gold nuclei interactions with emulsion nuclei at 10.7*A* GeV. The relativistic QMD model, which is a straightforward extension of QMD to high energy, was formulated in a very sophisticated way from the theoretical point of view, but its practical application to heavy-ion collisions is very complicated because of too much computing time.

Recently, we have developed a framework of Glauber plus QMD model (in short, DQMD model) that can be applied at high energy. The DQMD model suggests that the reaction process could be divided into two parts, the direct reaction and dynamical formation of highly-excited fragments. The direct reaction process is treated using the classical Glauber approach [14]. The dynamical aspect of collisions is followed by utilizing the QMD model [15]. These two processes are assumed to be well separated in their time scale with energies well above several *A* GeV. It was shown [16] that this framework could reproduce the measured nucleon invariant and double differential cross sections at $\geqslant$3*A* GeV. The success obtained in the previous studies has shown the ability of the DQMD approach for the study of the nucleon and heavy-ion induced nuclear reactions. However, the previous analysis has been concentrated on the inclusive particle spectra, and a fine selection of the final reaction products was not performed. It is, therefore, the purpose of this work to carry out an analysis of heavy-ion induced reactions for the production of the specific final states, i.e., fragments, with the same formula and the same set of parameters as the previous work to investigate further the validity of the DQMD approach.

In order to study the fragment production we have to supplement the DQMD model with a statistical decay code. Among the statistical models [17–19], we adopt the version of Ref. [17].

In this work, we analyze the data of the collision of 10.7*A* GeV gold nuclei on emulsion taken by the EMU-01 Collaboration [20]. The experimentally observed correlations between charged particles are represented as a function of Z_{b3}, which is the sum of the charges of fragments with charge $Z\geqslant 3$. This quantity depends on the size and also on the excitation energy of the decaying projectile spectator system and is expected to decrease with the centrality of the collision event. It was found [6,7,20] that several distinct charge correlations, such as the average maximum charge, $\langle Z_{\max}\rangle$, the intermediate mass fragment (IMF) multiplicity, $(3\leqslant Z\leqslant 30)$, the asymmetry of the largest to second largest charge, (A_{12}), the asymmetry of the second to third largest charge, (A_{23}), plotted as a function of Z_{b3} are almost independent of the chosen target and the measured techniques. This offers the possibility of inspecting pure ^{197}Au fragmentation at 10.7*A* GeV and hence cause interest in theoretical studies.

An analysis involving the same ingredients was made in Ref. [20] using a cascade [21] plus statistical decay (SD) model [17]. The basic difference between this combined model and the present approach is that the dynamical evolution of fragments after the first fast stage of the interaction is absent in the former model. Thus the comparison between the two models will allow us to disentangle the role of dynamics in MF.

This paper is organized as follows. In Sec. II, we define the basic ingredients of DQMD plus SD model, and discuss how these two are combined. In Sec. III, we compare the various fragment correlations calculated by this combined

*Present address: Umm Al-Qura University, Faculty of Applied Science, Physics Department, P.O. Box 6924, Makkah, Saudi Arabia. Electronic address: KHELWAGD@FRCU.EUN.EG

model with the experimental data of ^{197}Au fragmentation on emulsion nuclei at 10.7*A* GeV. Concluding remarks and a summary are given in Sec. IV.

II. DESCRIPTION OF DQMD PLUS SD MODEL

In this section, the original QMD model of Ref. [15] is supplemented with a Glauber's scattering recipe. The Glauber approach is used to determine the primary interacting or ''wounded'' nucleons and the location of these nucleons. Glauber scattering amplitudes and cross sections are calculated using wave functions which are applied by the QMD model. The dynamical aspects of collisions of the wounded and spectator nucleons of the target nucleus are treated by utilizing the QMD model. Aiming to establish a simple standard model, we have chosen the standard type of QMD model. For the SD process, we choose the one adopted by several papers [20,22,23] when studying the fragmentation of ^{197}Au at different energies ($\geqslant 600A$ MeV).

Initially, each nucleon (denoted by a subscript i) is represented by a Gaussian wave packet of constant width L (2 fm^2):

$$\phi(\vec{r}_i)=\frac{1}{(2\pi L)^{3/4}}\exp\left[-\frac{1}{4L}(\vec{r}_i-\vec{R}_i)^2+\frac{i}{\hbar}(\vec{r}_i\cdot\vec{P}_i)\right], \quad (1)$$

where $\vec{R}_i$ and $\vec{P}_i$ correspond to the centers of a wave packet in the coordinate and momentum spaces, respectively. The total wave function is assumed to be a direct product of these wave functions. The ground state of the nucleus is generated by packing $\vec{R}_i$ and $\vec{P}_i$ randomly in a sphere of radius R. The frictional cooling method [24] is applied to find the ground state configurations, which allows to reproduce very well the experimental values of the ground state binding energies and root mean square radii of the nuclei.

The Wigner transform of the wave function of nucleus A has the form

$$F(\vec{r}_1,\vec{r}_2,\ldots,\vec{r}_A,\vec{p}_1,\vec{p}_2,\ldots,\vec{p}_A)=\sum_{i=1}^{A} f(\vec{r}_i,\vec{p}_i),$$
$$f(\vec{r}_i,\vec{p}_i)=\frac{1}{(\pi\hbar)^3}\exp\left[-\frac{1}{2L}(\vec{r}_i-\vec{R}_i)^2-\frac{2L}{\hbar^2}(\vec{p}_i-\vec{P}_i)^2\right]. \quad (2)$$

Integrating over all momentum space yields the single-particle density,

$$\rho(\vec{r}_i)=\int\frac{d^3p_i}{(2\pi\hbar)^2}f(\vec{r}_i,\vec{p}_i)$$
$$=\frac{1}{(2\pi L)^{3/2}}\exp\left[-\frac{1}{2L}(\vec{r}_i-\vec{R}_i)^2\right]. \quad (3)$$

The single-particle density can be used in Glauber's theory to calculate the density of the nucleus:

$$\rho_A(\vec{r}_1,\vec{r}_2,\ldots,\vec{r}_A)=\prod_{i=1}^{A}\rho(\vec{r}_i)=|\psi_A(\vec{r}_1,\ldots,\vec{r}_A)|^2, \quad (4)$$

where $\psi_A(\vec{r}_1,\ldots,\vec{r}_A)$ is the total wave function of the nucleus A.

In the Glauber's approach, the cross section of inelastic interaction of nucleus A on nucleus B is given by the expression,

$$\sigma_{AB}^{\text{in}}=\int d^2b\left\{1-\prod_{i=1}^{A}\prod_{k=1}^{B}(1-p(\vec{b}-\vec{s}_i+\vec{\tau}_k))\right\}$$
$$\times|\psi_A(\vec{r}_1,\ldots,\vec{r}_A)|^2\prod_{i=1}^{A}d^3r_i|\psi_B(\vec{t}_1,\ldots,\vec{t}_B)|^2\prod_{i=1}^{B}d^3t_i, \quad (5)$$

where

$$p(\vec{b})=\gamma(\vec{b})+\gamma^*(\vec{b})-\gamma(\vec{b})\gamma^*(\vec{b}).$$

In Eq. (5), $\vec{b}$ is the impact parameter and γ is the amplitude of elastic nucleon-nucleon (NN) scattering in the impact parameter representation. $\vec{s}_j$, $j=1,2,\ldots,A$ and $\vec{\tau}_k$, $k=1,2,\ldots,B$ are projections of the coordinates of nucleons of nucleus A and B on impact parameter plane, respectively.

Equation (5) can be rewritten in a form where each of the terms would be interpreted as a probability of some process

$$\sigma_{AB}^{\text{in}}=\int d^2b\left\{\sum_{i=1}^{A}\prod_{j=1}^{B}\frac{p(\vec{b}-\vec{s}_i+\vec{\tau}_j)}{1-p(\vec{b}-\vec{s}_i+\vec{\tau}_j)}\right.$$
$$\times\prod_{k=1}^{A}\prod_{l=1}^{B}(1-p(\vec{b}-\vec{s}_k+\vec{\tau}_l))$$
$$+\frac{1}{2}\sum_{\substack{i=1,j=1\\ i\neq j}}^{A}\sum_{k=1}^{B}\frac{p(\vec{b}-\vec{s}_i+\vec{\tau}_k)}{1-p(\vec{b}-\vec{s}_i+\vec{\tau}_k)}\frac{p(\vec{b}-\vec{s}_j+\vec{\tau}_k)}{1-p(\vec{b}-\vec{s}_j+\vec{\tau}_k)}$$
$$\left.\times\prod_{l=1}^{A}\prod_{m=1}^{B}(1-p(\vec{b}-\vec{s}_l+\vec{\tau}_m))+\cdots\right\}$$
$$\times|\psi_A(\vec{r}_1,\ldots,\vec{r}_A)|^2\prod_{i=1}^{A}d^3r_i|\psi_B(\vec{t}_1,\ldots,\vec{t}_B)|^2\prod_{i=1}^{B}d^3t_i. \quad (6)$$

Here the first term in braces is interpreted as a probability that the only one inelastic collision between ith nucleon from nucleus A and jth nucleon from nucleus B takes place when all nucleons coordinates and impact parameter are fixed. The second term describes a probability of inelastic collision of the kth nucleon from nucleus B with ith and jth nucleons in A nucleus, etc. The nucleons involved in these collisions are identified as ''wounded,'' all others are ''spectators.''

The interpretation is true, if the function $p(\vec{b})$ is positive which is satisfied at high energy. In this case, the *NN* elastic scattering amplitude is parametrized as

$$\gamma(\vec{b})=\sigma_{NN}^{\text{tot}}\frac{1-i\alpha}{4\pi B'}e^{-\vec{b}^2/2B'}. \quad (7)$$

Here $\sigma_{NN}^{\rm tot}$ is total cross section of *NN* interaction, α is ratio of real part to imaginary part of elastic scattering amplitude at zero momentum transfer, and B' is the slope parameter of differential cross section of elastic *NN* scattering. At 10.7*A* GeV, these values are taken as [20] $\sigma_{NN}^{\rm tot}=40$ mb, $\alpha=0.0$, and $\beta=12.84\,({\rm GeV}/c)^2$.

According to Ref. [14], the determination of wounded nucleons is carried out through the following steps:

(1)Sampling of impact parameter according to Glauber approach;

(2)Sampling of the nucleon coordinates according to $|\psi_A(\vec{r}_1,\ldots,\vec{r}_A)|^2$ and $|\psi_B(\vec{r}_1,\ldots,\vec{r}_B)|^2$;

(3)Sampling of the elementary interactions: the ith nucleon of the nucleus A can interact with jth nucleon of nucleus B with probability $p(\vec{b}-\vec{s}_i+\vec{\tau}_j)$.

It is obvious that the primary interacting wounded nucleons accept momentum and can be escaped from the nucleus. To take this into account, we ascribe to each wounded nucleon a transverse momentum distributed according to the law

$$dP' \sim \prod_{i=1}^{N_w} e^{-(p'^2_{i\perp}/\langle p_\perp^2\rangle}\delta\left(\sum_{i=1}^{N_w} p'_{i\perp}\right) dp'_{i\perp}, \tag{8}$$

where N_w is the number of wounded nucleons and $\langle p_\perp^2\rangle = 500\,({\rm MeV}/c)^2$.

The additional longitudinal momentum distribution is chosen as

$$dP' \sim \prod_{i=1}^{N_w} e^{-(p'_{iL}-d)^2/\langle p_L^2\rangle}\delta\left(\sum_{i=1}^{N_w} p'_{iL}\right) dp'_{iL}, \tag{9}$$

where $d=700\,({\rm MeV}/c)$ and $\langle p_L^2\rangle = 500\,({\rm MeV}/c)^2$. The momentum components of Eqs. (8) and (9) are added to the primary nucleon momentum ($\vec{P}_i \to \vec{P}_i+\vec{P}'_i$). The R space of each wounded nucleon of the target nucleus is then modified by $\vec{R}_i \to \vec{R}_i+(\vec{P}_i/E_i)\tau$, where E_i is its energy. τ is defined as the time necessary for the wounded nucleon to interact with other spectator nucleon. This is a free parameter of the model and fixed (at $\tau=1$ fm/c) from the requirement of best description of the available experimental data for proton-nucleus collisions at energy of 3.7 GeV [16].

In principle, the distributions of Eqs. (8) and (9) can be obtained using different methods. For example, one can deduce them from *NN*-interaction data. The Monte Carlo generators of artificial events (e.g., FRITIOF [25], relativistic QMD [12],...) can also be applied. In this paper we restrict ourselves to the simplest parametrization.

The spectator nucleons are assumed to have the same coordinates and momenta as the cooled nucleus.

After the first fast stage of the interaction, the time evolution of the spectator and wounded nucleons of the target nucleus is assumed to proceed in a relatively low energy regime where nonrelativistic mean field can be applied. The time evolution is described by Newtonian equations and the stochastic two-body collision terms. The Newtonian equations are derived on the basis of the time dependent variation principle as

$$\frac{dR_j}{dt}=\frac{\partial H}{\partial P_j}, \quad \frac{dP_j}{dt}=-\frac{\partial H}{\partial R_j}, \tag{10}$$

where the Hamiltonian H consists of the single particle energy including mass term and energy of the two-body interaction. As for the effective interaction, we adopt the Skyrme-type, Coulomb, and momentum dependent Pauli terms. By using the Gaussian function of nucleons (2) we obtain

$$\begin{aligned} H=&\sum_j \sqrt{m_j^2+p_j^2}+\frac{\alpha}{2\rho_0}\sum_{i=1}^{A}\sum_{\substack{k=1\\k\neq i}}^{A}\tilde{\rho}_{ik} \\ &+\frac{\beta}{(\gamma+1)\rho_0^\gamma}\sum_{i=1}^{A}\left(\sum_{\substack{k=1\\k\neq i}}^{A}\tilde{\rho}_{ik}\right)^\gamma+\frac{\omega}{2\rho_0}\sum_{i=1}^{A}\sum_{\substack{k=1\\k\neq i}}^{A}\xi_i\xi_k\tilde{\rho}_{ik} \\ &+\frac{G}{8L^2}\sum_{i=1}^{A}\sum_{\substack{k=1\\k\neq i}}^{A}(6L-r_{ik}^2)\tilde{\rho}_{ik} \\ &+\frac{1}{2}V_0^P\frac{\hbar^2}{16\,{\rm mL}^2}\sum_{i=1}^{A}\sum_{\substack{j=1\\j\neq i}}^{A}\frac{Q_{ij}^2}{e^{1/4LQ_{ij}^2}-1}\delta_{t_it_j}\delta_{s_is_j} \\ &+\frac{1}{2}e^2\sum_{i=1}^{A}\sum_{\substack{j=1\\j\neq i}}^{A}\frac{1}{r_{ij}}{\rm erf}\left(\frac{r_{ij}}{2\sqrt{L}}\right), \end{aligned} \tag{11}$$

where

$$\vec{r}_{ik}=\vec{R}_i-\vec{R}_k,$$

$$\xi_i=\begin{cases}+1 \text{ for protons,}\\ -1 \text{ for neutrons,}\end{cases}$$

the phase-space distance $Q_{ij}^2=(\vec{R}_i-\vec{R}_j)^2+4L^2/\hbar^2(\vec{P}_i-\vec{P}_j)^2$,

and the ''interaction density'' $\tilde{\rho}_{ik}=\frac{1}{(4\pi L)^{3/2}}e^{-1/4L(\vec{R}_i-\vec{R}_k)^2}$.

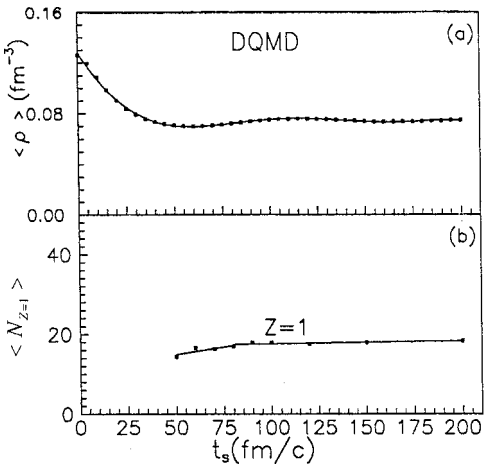

FIG. 1. Evolution of the Au fragmentation at 10.7*A* GeV on emulsion as calculated by the DQMD model. (a) Displays the time evolution of the average density. (b) The time evolution of the single charged fragments emitted at the fast stage of the interactions.

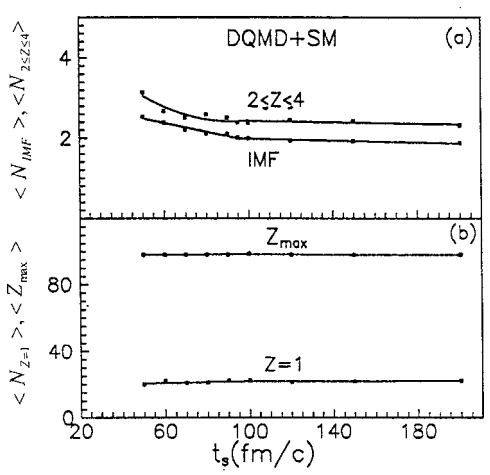

FIG. 2. Evolution of the ^{197}Au fragmentation on emulsion at 10.7*A* GeV as calculated by the DQMD plus SD model. (a) The dependence of the heaviest fragments $\langle Z_{\max}\rangle$ and the single charged fragments $\langle Z=1\rangle$ on the switching time t_s. (b) The same as (a), but for the light-charged fragments ($2\leqslant Z\leqslant 4$) and IMF's ($\langle 3\leqslant Z \leqslant 30\rangle$).

The summation runs over all spectator and wounded nucleons of the target nucleus and erf denotes the error function. The values of the potential parameters appearing in Eq. (11) are chosen to be $\alpha=-356$ MeV, $\beta=306.1$ MeV, $\gamma=1.1667$, $w=30.54$ MeV, $G=291.0$ (MeV fm^5), and $V_0^P=1.9$, which correspond to the soft equation of state (EOS) with compressibility $K=200$ MeV, saturation at $\rho=\rho_0=0.168$ fm^{-3}, and a binding energy of 16 MeV per nucleon for infinite nuclear matter. We use another parameter set of the Skyrme-type force to describe the hard EOS. These parameters are $\alpha=-124.69$ MeV, $\beta=74.24$ MeV, $\gamma=2$, which correspond to compressibility $K=380$ MeV. It should be noted here that the ground state binding energies and root mean square radii of the nuclei in ground state are quite well reproduced by the potential with the specified parameters. These values are taken from Ref. [24].

The sampling of particle interactions of the wounded and spectator nucleons of the target nucleus is made at each time step. Any two nucleons become candidates for scattering if their spatial distance r_{ij} is less than the interaction distance $d_{\rm int}$. If there are such nucleons, the new momenta are determined assuming isotropic scattering. The collision is allowed if the new states are not already occupied by like nucleons. Otherwise, the collision is blocked and the two nucleons continue their movement in the effective potential. For the sake of numerical feasibility, the *NN* cross section is assumed to be constant ($\sigma_{NN}=40$ mb).

It should be mentioned that the procedure described above can equally be applied for the projectile nucleus in its rest frame.

The DQMD calculation is carried out up to a time scale, which is referred to as the switching time, t_s. The position of each nucleon is then used to calculate the distribution of mass and charge numbers (refereed to as ''prefragments''). In determining the mass and charge numbers of the prefragments, the minimum spanning tree method [11] is employed, a prefragment is formed if the centroid distances are lower than 3 fm. The excitation energy of the hot prefragments is calculated as a difference between the binding energy of the hot prefragments and the binding energies of these prefragments in their ground state.

The ensemble of prefragments is characterized by excitation energy E^*, nucleon *A*, and proton *Z* numbers. The decay of the residual nuclei is described by the SD model [17]. The SD model assumes that a hot nucleus expands to a freeze-out volume, where it splits into primary hot prefragments and nucleons in thermal equilibrium. Obviously, the volume is a free parameter of the model. The volume is generally [17] defined as $V_b=(1+k)V_0$, $k\sim 2-3$, and V_0 is the volume of *A* nucleons system in the ground state. As in Ref. [3], the value of $k=2$ is used. The breakup channels are constrained by the total mass, charge, and energy of the system. All prefragments (and nucleons) are considered as Boltzmann particles while Fermi gas approximation is used for their internal excitation. The probabilities of different breakup channels are calculated micronically, according to their statistical weights. After primary breakup excited prefragments propagate independently under mutual Coulomb field and undergo secondary decay described by evaporation, Fermi breakup, or fission, depending on their mass and excitation energy. The simulation of the whole process is performed by the Monte Carlo method.

The separation of the DQMD and SD calculations introduces an ambiguity because the switching time, t_s, is an arbitrary parameter. To resolve this ambiguity, we have carried out the DQMD calculations without (Fig. 1) and with (Fig. 2) SD model by changing the value of t_s, and investigated how the results would vary as a function of t_s. In the simulation, a soft EOS for 1000 events is employed. Figures 1 and 2 display the results for Au fragmentation on emulsion at 10.7*A* GeV. The first row of Fig. 1 shows the density averaged over the centroid of all nucleons:

$$\langle \rho \rangle = \frac{1}{A} \sum_{i}^{A} \rho(R_i),$$

$$\rho(\vec{R}_i) = \frac{1}{(2\pi L)^{3/2}} \sum_{j=1}^{A} \exp\left[-\frac{1}{2L} (\vec{R}_i - \vec{r}_j)^2 \right],$$

where R_i being the centroid position of the nucleon (i). One finds that the average density attains an asymptotic value at $t_s \sim 50$ fm/c. The second row of Fig. 1 shows the time evolution of the emitted singly charged particles after the first fast stage of the interaction. As one can see, we have stable singly charged emission at $t_s \geqslant 90$.

However, this does not necessarily mean that these values are also appropriate to obtain stable values for more exclusive observables as the fragment production. Therefore, we have carried out calculations by changing the value of t_s, and investigated how various fragment production would vary as a function of this parameter. The result is shown in Fig. 2 for the production of single charged fragments, $\langle N_{Z=1} \rangle$, light charged fragments, $\langle N_{2 \leqslant Z \leqslant 4} \rangle$, $\langle N_{\mathrm{IMF}} \rangle$, and $\langle Z_{\max} \rangle$. This is a result of the DQMD plus SD calculation. One notices that the heaviest fragments are formed rather early. This gives an indication that the heaviest fragment is formed from the spectator matter and not by coalescence, a conclusion that is supported by the analysis of Ref. [26]. The single charged fragments, light charged fragments, and IMF's, however, need a longer time (about 95 fm/c) until it can be stable. Thus, in what follows, we will define the switching time in a unique way at $t_s = 100$ fm/c.

III. DATA VERSUS DQMD PLUS SD PREDICTIONS

We have performed a calculation of fragmentation of Au projectiles after collisions with emulsion nuclei [emulsion is the composition of the following nuclei: H(3.76%), C(17.80%), O(4.70%), N(13.60%), Br(13.10%), and Ag(13.10%)] at a bombarding energy of 10.7A GeV. The results of DQMD plus SD model are presented in Figs. 3 and 4 with soft (solid histograms) and hard (short dashed histograms) EOS parameters. Calculations with event number of 10 000 for each EOS have been performed. The impact parameter has been calculated according to Glauber approximation [14]. The comparisons shown in Figs. 3 and 4 are based on the data reported in Ref. [20]. There, the data are analyzed in terms of two quantities, Z_{b2} and Z_{b3}, which differ by the sum of fragments with $Z=2$. It is experimentally verified that the use of Z_{b3} instead of Z_{b2} makes possible the discriminations between the mechanisms at high (10.7A GeV) and intermediate (600A MeV [7] and 1000A MeV [6]) energies. Thus we are going to study the fragment correlations as a function of Z_{b3}.

Figure 3(a) shows the dependence of the single-charged multiplicity, $\langle N_{Z=1} \rangle$, on Z_{b3} together with the predictions of the DQMD plus SD model for soft and hard EOS. The single charged fragments are calculated from the deexcitation of the hot prefragments. As one can see, the combined model slightly underestimates the single-charged fragments as a function of Z_{b3}. As was pointed out in Ref. [20], the reason

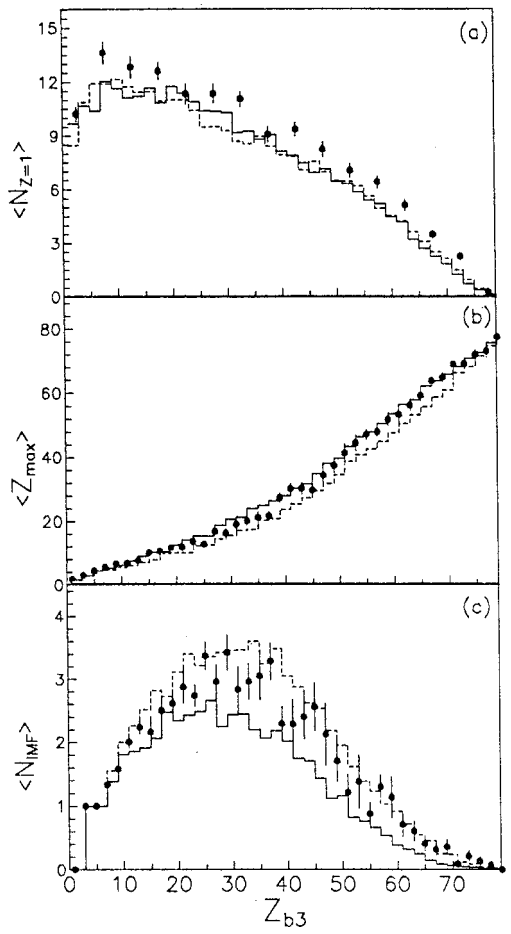

FIG. 3. Average multiplicity of single charged fragments $\langle N_{Z=1} \rangle$ (a), the heaviest fragments $\langle Z_{\max} \rangle$ (b), and the IMF's $\langle N_{\mathrm{IMF}} \rangle$ (c) as a function of Z_{b3}, as obtained from the DQMD plus SD calculations with soft (solid histograms) and hard (dashed histograms) EOS in comparison to the experiment (closed circles) from Ref. [13].

for this discrepancy may be due to the fact that the single-charged fragments selected by conventional emulsion techniques are distorted by multiparticle production at the first fast stage of the interaction. There is no significant difference between soft and hard EOS predictions in the whole range of Z_{b3}.

In Fig. 3(b) the average charge distribution of the heaviest fragment in an event as a function of Z_{b3} is presented. As can be seen, the DQMD plus SD calculations with the soft EOS remarkably reflect the characteristics of the heaviest fragment in an event. The average charge of the heaviest fragments for $Z_{b3} > 16$ obtained using the combined model calculations with the hard EOS is smaller than that of the soft ones.

Figure 3(c) gives the average values of IMF as a function of Z_{b3}. One learns from this figure that the average multiplicity of the IMF increases first with the decrease of Z_{b3} (i.e., with the decrease of impact parameter) and then starts to decrease after reaching a maximum at $Z_{b3} = 25 - 35$. It can also be seen from the figure that the hard EOS leads to IMF multiplicity values $\sim$40% larger than the soft EOS in the

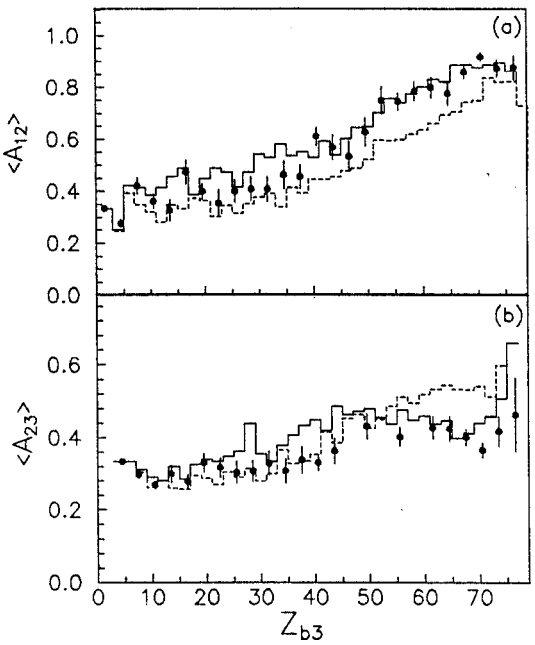

FIG. 4. Same as Fig. 3, but for the first asymmetry $\langle A_{12}\rangle$ (a) and the second asymmetry $\langle A_{23}\rangle$ (b) as a function of Z_{b3}.

range $25<Z_{b3}<30$. Note that this leads to breaking the heavy fragments into a large number of IMF's in peripheral collisions [for $Z_{b3}>25$, see Fig. 3(b)]. This may imply that the model nuclei for the soft EOS seem to be much more fragile than the ones for hard EOS.

In Fig. 4, we compare the average asymmetry parameters used to characterize the three heaviest fragments in the event. The first asymmetry of fragments A_{12} and the second asymmetry A_{23} are defined, respectively, as

$$A_{12}=\frac{Z_{\max}-Z_2}{Z_{\max}+Z_2}$$

and

$$A_{23}=\frac{Z_2-Z_3}{Z_2+Z_3},$$

where Z_2 and Z_3 are the charges of the second and third heaviest fragment, respectively. This figure shows clearly that the two asymmetry parameters decrease smoothly with the decrease of Z_{b3}, and can be reproduced beautifully (within the error bars) by the combined model with the soft EOS.

From Figs. 3 and 4, it is clear that the aforementioned quantities, especially $\langle N_{\rm IMF}\rangle$, $\langle A_{12}\rangle$, and $\langle A_{23}\rangle$ as a function of Z_{b3}, are sensitive to different EOS at peripheral collisions (with the increase of Z_{b3} values). This difference is encouraging as it can give a clue about the EOS in nuclear matter. On the other hand, the dependencies of $\langle N_{\rm IMF}\rangle$, $\langle A_{12}\rangle$, and $\langle A_{23}\rangle$ on Z_{b3} for soft and hard EOS are practically in coincidence at $Z_{b3}<16$; although the excitation energy difference between the calculation results with the two different states in this region is maximum (see Fig. 5). It is also reported, in Ref. [27], that the data points for Kr(900*A* MeV) and Au(10.7*A* GeV) fragmentation residues are close to each other in this particular region. This indicates that for very central collisions, the remaining 20% of the residual nuclei that survived from different interactions will fragment (at a given excitation energy) in a manner independent of both the excitation energy and the mass number of the projectile.

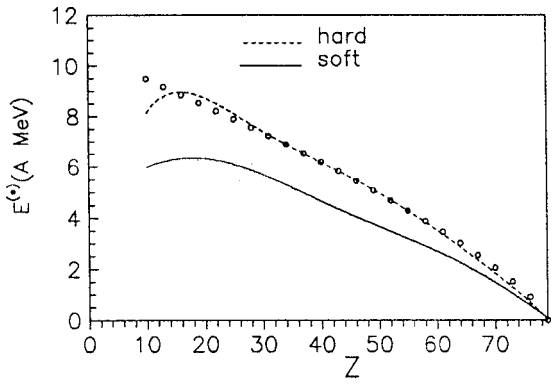

FIG. 5. The excitation energy per nucleon E^* as a function of the prefragment charge Z in the interactions of Au on emulsion at 10.7*A* GeV. The dotted line represents the DQMD calculations with the hard EOS, whereas the solid line represents the calculations with the soft EOS. Open circles display the parametrization of Ref. [13].

It should be pointed out here that, in Ref. [20], a type of cascade models is used to analyze the correlations presented in this work. This model is very similar to ours in the very fast and last stages of the interactions, where in the former stage of the interaction they treated the primary interacting nucleons by the same Glauber approach, while in the latter stage the decay of the excited residues is treated using the same SD model. It is shown that the excitation energy of the resulting source sizes could not properly be defined from the cascade simulations. A similar conclusion is also drawn in Refs. [28,29], when they studied the fragmentation of ^{197}Au at 600*A* MeV. A correction of the excitation energy calculations has to be taken into account. In Ref. [20], the excitation energy is adjusted so as to reproduce the average values of IMF multiplicities. In Fig. 5, the open circles represent their parametrization. The source sizes and excitation energies extracted using the DQMD model are also displayed for soft (solid line) and hard (dotted line) EOS. As one can see, their parametrization is compatible with the DQMD calculations for the hard EOS. It is found that the data are, by far, not so well described in Ref. [20] as they are in the present work, even for the hard EOS parameters. This may imply that the dynamics [propagation of nucleons through the mean field of Eq. (11) and *NN* stochastic scattering] play a very important role in determining both the correct excitation energies and fragment sizes.

IV. SUMMARY AND CONCLUSIONS

In this work, we have studied the fragmentation of ^{197}Au at 10.7*A* GeV. The fragment correlations as a function of Z_{b3} are compared by a multistep model. The combined model suggests that the reaction processes proceed through three

stages, i.e., the direct reaction, the dynamic, and the statistical decay. In the direct reaction, the distribution of nucleons knocked out by hard collisions are calculated according to classical Glauber approach. The dynamics, which is governed by the propagation of nucleons through the mean field and stochastic two body collisions, are treated using standard QMD model. The highly excited fragments, that are formed (at 100 fm/c) at the end of this stage, allowed to disassemble via a statistical decay code. From such comparison the following conclusions can be drawn:

(i) The combined model with the soft EOS yields a better description of the ^{197}Au fragmentation at 10.7A GeV, than that with the hard EOS.

(ii) The difference between soft and hard EOS is sizable at peripheral collisions (large Z_{b3} values). This suggests that the fragmentation study in this region plays an important role in determining the nuclear EOS.

(iii) The excitation energy levels off for $Z_{b3}<16$ at $\sim 6A$ MeV, suggesting limiting fragmentation in central collisions.

(iv) Collision events with $Z_{b3}\sim 30$ and excitation energies of 5.5A MeV and 6.5A MeV for soft and hard EOS, respectively, give rise to most of the IMF's produced.

(v) The Glauber plus QMD model is a useful approach for the high energy ($\geqslant 3A$ GeV) heavy-ion reactions and gains an advantage over the cascade model and the like that need a lot of adjustable parameters.

Thus the study of the DQMD model showed that this is a promising direction to generalize the QMD simulations to high energy. The systematic calculation of the DQMD model, however, is now in a beginning stage. For example, we need to take care of multiparticle production at the first fast stage of the interactions. At high energy ($\geqslant 10.7A$ GeV) a large number of pions should be produced in primary NN interactions, and their evolution inside the system may influence the distribution of excitation energy in its interior. The study in this direction is in progress.

[1] P. Krenz *et al.*, Nucl. Phys. **A556**, 672 (1993).
[2] W.-C. Hsi *et al.*, Phys. Rev. C **60**, 034609 (1999).
[3] M. I. Adamovich *et al.*, EMU01 Collaboration, Eur. Phys. J. A **1**, 77 (1998).
[4] M. L. Cherry *et al.*, KLMM Collaboration, Phys. Rev. C **52**, 2652 (1995).
[5] W. Reisdorf *et al.*, FOPI Collaboration, Nucl. Phys. **A612**, 493 (1997).
[6] A. Schttauf *et al.*, Nucl. Phys. **A607**, 457 (1996).
[7] A. S. Botvina *et al.*, Nucl. Phys. **A584**, 737 (1995).
[8] V. D. Tonnev and K. K. Gudima, Nucl. Phys. **A400**, 173 (1983).
[9] J. Cugnon, C. Volant, and S. Vuiller, Nucl. Phys. **A620**, 575 (1997).
[10] W. Bauer, Phys. Rev. Lett. **61**, 2534 (1988).
[11] Ch. Hartnack, Rajeev K. Puri, J. Aichelin, J. Konopka, S. A. Bass, H. Stöcker, and W. Greiner, Eur. Phys. J. A **1**, 151 (1998).
[12] H. Sorge, H. Stöcker, and W. Greiner, Nucl. Phys. **A498**, 567c (1989).
[13] M. I. Adamovich *et al.*, EMU01 Collaboration, Z. Phys. A **358**, 357 (1997).
[14] S. Yu. Shmakov, V. V. Uzhinskii, and A. M. Zadorozhny, Comput. Phys. Commun. **54**, 125 (1989), and references therein.
[15] J. Lukasik, Z. Majka, and T. Kozik, Phys. Lett. B **318**, 419 (1993).
[16] Kh. Abdel-Waged, A. Abdel-Hafiz, and V. V. Uzhinskii, J. Phys. G **26**, 1105 (2000).
[17] J. B. Bondorf *et al.*, Phys. Rep. **257**, 134 (1995).
[18] D. H. E. Gross, Rep. Prog. Phys. **53**, 3605 (1990).
[19] V. Weisskopf, Phys. Rev. **52**, 295 (1937); W. A. Friedmann, Phys. Rev. C **28**, 16 (1983).
[20] M. I. Adamovich *et al.*, EMU01 Collaboration, Z. Phys. A **359**, 277 (1997).
[21] Khaled Abdel-Waged, Phys. Rev. C **59**, 2792 (1999).
[22] H. W. Barz, W. Bauer, J. B. Bondorf, A. S. Botvina, R. Donangelo, H. Schulz, and K. Sneppen, Nucl. Phys. **A561**, 466 (1993).
[23] Hongfei Xi *et al.*, Z. Phys. A **359**, 397 (1997).
[24] D. H. Boal and J. N. Glosli, Phys. Rev. C **38**, 1870 (1988); **38**, 2621 (1988).
[25] B. Andersson *et al.*, Nucl. Phys. **B281**, 289 (1987).
[26] R. Donangelo and S. R. Souza, Phys. Rev. C **58**, R2659 (1998).
[27] A. Abd-Elhafiez, M. M. Chernyavski, K. G. Gulamov, V. Sh. Navotny, G. I. Orlova, and V. V. Uzhinskii, Phys. At. Nucl. (to be published); (private communications).
[28] A. S. Botvina and I. N. Mishustin, Phys. Lett. B **294**, 23 (1992).
[29] Z. Yu-Ming, W. Fei, S. Ben-Hao, and Z. Xiao-Ze, Phys. Rev. C **53**, 1868 (1996).